Deciphering the effect of sea water on corrosion behavior of epoxy/graphite-flakes composite coated LDX 2101 stainless steel.

Jitendra Chavhan[1] and Tushar R. Dandekar [2]*

(1) Jitendra Chavhan [1]

E-mail: jitu.chavhan29@gmail.com

Affiliation(s): [1]Department of Metallurgical and Materials Engineering, Visvesvaraya National Institute of Technology (VNIT), South Ambazari Road, Nagpur - 440010, Maharashtra, India.

ORCID: orcid.org/0000-0001-6381-3234

(2) Tushar R. Dandekar [2] (*Corresponding author)

E-mail: tushar.dandekar3@gmail.com

Affiliation(s): [2]School of Mechanical and Design Engineering, University of Portsmouth Anglesea building, Room 2.09, Anglesea Road, Portsmouth, PO1 3DJ Hampshire, United Kingdom

Phone No: +447909020390, +919175389593,

ORCID: orcid.org/0000-0003-2391-0835

Abstract

In the present investigation, the electrochemical behaviour of lean duplex stainless steel (LDX 2101 SS) and epoxy (EP) coated with and without containing graphite flakes in a marine or seawater environment (3.5 wt% NaCl) was studied. The epoxy/graphite flakes (EGF) coating was prepared using a spin coater, and then the morphological and physical properties of the coating were analysed by scanning electron microscopy (SEM) and water contact angle (WCA). The performance of EP and EGF composites as protective coatings against corrosion of LDX 2101 was analysed using electrochemical impedance spectroscopy (EIS) and potentiodynamic polarization techniques. The final result shows that EGF composite has excellent corrosion protective ability compared to bare and epoxy-coated steel.

Keywords: Epoxy**,** corrosion, graphite flakes, coating, LDX2101

1. Introduction

Industrialists and scientists are deeply concerned about the tendency of steel to corrode, such as 304, 316, 201 low nickel austenitic stainless steel, and LDX 2101 duplex stainless steel series [1, 2]. Metal corrosion caused by the interaction of materials and mediums (electrolytes) has been responsible for a number of industrial disasters and needs to be addressed using new materials and methods. Because of the ongoing use of oil and natural gas resources on land, people are increasingly interested in resources lying beneath the sea. Extreme hydrostatic pressure, low temperatures and intensely corrosive marine environments offer enormous issues for pipeline engineering services. Due to its availability, affordable price, great corrosion resistance, and superior biosafety, 316L SS has historically been used to construct deep sea oil pipelines [3, 4]. However, owing to its superior corrosion resistance and affordable price, LDX 2101 is currently gaining demand as a better alternative to 316L SS. Steel pipes have a number of issues in a marine environment, including pitting corrosion, according to field statistics data [5]. In addition to cathodic protection, coatings are now being developed to capitalize on the exposed surface and enhance the materials' resistance to corrosion at affordable prices.

On the other hand, the use of polymeric coatings for the production of inexpensive corrosion protective barriers has attracted lots of interest. Due to its exceptional toughness, adherence to metal substrates, and longevity, epoxy coatings have become extensively used coatings to shield metal structures against atmospheric and corrosion threats. However, the epoxy coatings are being penetrated by water and electrolytic species and may degrade with time. Epoxy coatings with dispersing fillers have been created as a result to improve the anticorrosive capabilities of metals [6-8].

Pure carbon exists in the form of graphite, which is crystalline and closely resembles the firmly linked mica sheets. Nevertheless, because of its porosity, graphite functions as a perfect dry lubricant at ambient temperatures. It is made up of a structure in which the carbon atoms are connected by covalent bonds with other carbons in the same plane formed by the Van Der Waals force operating between consecutive layers. The layers of graphite should be removed and dispersed throughout the polymeric matrix for efficient usage as stuffing in a polymeric composite [9-12].

It is found that the addition of nanofillers improves the properties of the epoxy matrix; for example, by using high temperature milling processes, iron oxides have been introduced to the coating to reduce imperfections at the interface between the epoxy and the metal substrate [13]. It was reported that TiO_2 nanoparticle-infused epoxy coatings were used to enhance the

coatings' mechanical and anticorrosion characteristics [14]. According to the authors best knowledge, there is no study presently available in the literature that studies the effect of corrosion on LDX 2101 with and without coatings for marine pipeline applications. Thus, in this work, our motivation is to study the influence of sea water (3.5 wt% NaCl) on LDX 2101 for anticorrosive applications with and without Epoxy/Graphite flakes (EGF) coating. Therefore, graphite flakes were used as an anticorrosive pigment in epoxy coatings.

2. Experimental

Graphite flakes powder of 10–20 microns, Epoxy resin (E44), Sodium chloride (NaCl, purity: 99.9 %), 256S DuPont Activator fast (Hardner), Acetone (purity: 99 %), Deionised water, LDX 2101 is used in the present work and Fig. 1(a) shows schematic of fabrication of EGF coating. Further details related to experimental section are provided in Electronic Supplementary Material as "2.1 Fabrication of EGF coating" and "2.2 Instrumentations".

3. Results and discussion

3.1. Morphological and structural analysis of powdered graphite flakes (GF)

Fig. 1(b, c) shows the scanning electron microscope (SEM) images of GF, which has a particularly flaky or platy shape. On some level, all graphite has a flaky morphology, but generally, GF has this structure independent of particle size. Fig. 1d shows the X-ray diffraction (XRD) pattern of GF. The presence of sharp peaks represents the crystalline structure of GF, a high intensity XRD peak at $2\theta = 26.5°$ and a low intensity peak at $2\theta = 54.5°$ were explicit to the (002) and (004) planes correspondingly [15]. Fig. 1e illustrates the Fourier transform infrared (FT-IR) spectra of GF powder. The results show that there are no functional groups on the surface of graphite powder. An obvious peak between 3000 cm^{-1} and 3600 cm^{-1} (with a central value of approximately 3429 cm^{-1}) is observed and is related to hydroxyl (OH) absorption or even the water adsorbed during the data acquisition. This peak is ascribed to the O-H stretching vibrational mode of intercalated water. The peak at 1639 cm^{-1} is allotted to the C=C model of graphitic nature. The absence of strong bands at 1213 cm^{-1} and 1053 cm^{-1} proposes the absence of any oxygenated groups like epoxy C–O–C or alcohol C–O [15].

3.2. Surface morphology and wettability of epoxy/graphite flakes (EGF) coated steel

Fig. 2a shows the SEM image and water contact angle (WCA) of EP and EGF coated SS surface to check the surface morphology and wettability. In SEM images, the EP coated surface

appears transparent and smooth, while the EGF coated surface appears darker and rougher, which could be due to the blackness of GF. Fig. 2b represents the WCA values of EGF coating that are higher than that of EP. This could be due to the fact that GF addition makes coating compact by reducing the pores and making it a little rough, which helps to keep low contact with water droplets.

3.3. Anticorrosion measurements of EGF coatings

The electrochemical studies, namely electrochemical impedance spectroscopy (EIS) and anodic polarization, were used to measure the anticorrosion properties of coatings in a 3.5 % NaCl solution. The EIS outcomes presented in the form of Nyquist plots and bode-phase angle plots for bare LDX 2101 and LDX 2101 coated with EP and EGF coatings are shown in Fig. 3. It is observed (Fig. 3a) that the EP and EGF coated SS shows a higher diameter of a semicircle in comparison with the bare LDX 2101 specifies the high resistance of the film [16]. The diameter of a semicircle of EP coated LDX 2101 improved significantly after incorporation of the graphite flakes and the best result is obtained in case of EGF coated LDX 2101. This result is further supported by the bode-phase angle plot. Fig. 3c-d shows that EGF coated LDX 2101 has high impedance values at low frequencies and a high phase angle over a large frequency range, which indicates that EGF coating has good anticorrosion properties [16]. The equivalent circuit model (Fig. 3(b)) used to fit the plots and obtain the results in terms of solution resistance (R_s), coating resistance (R_c), coating capacitance (CPE_c), charge transfer resistance (R_{ct}) and double layer capacitance (CPE_{dl}) are given in Table 1(a). The highest R_c, R_{ct} values and the lowest CPE_c, CPE_{dl} values were represented by the EGF coated sample compared to other samples indicating high resistiveness and low water absorption capability of coating [16]. The anticorrosion characteristics of coated samples can possibly be predicted using the WCA values. Higher WCA values suggest less potential for surfaces to corrode as a result of water repulsion, whereas lower WCA values reveal a tendency of water to spread and attach to the surface, leading to a greater inclination towards corrosion. Tafel plots of bare LDX 2101, EP and EGF coated sample are shown in Fig. 3e. Extrapolation of the Tafel plot consisting of corrosion current density (i_{corr}) and corrosion potential (E_{corr}) provided in Table 1(b) yields the associated polarisation parameters. It was noticed that EGF coated samples had higher E_{corr} and lower i_{corr} values than EP and bare samples. This demonstrates that the EGF coating functions as a barrier between the corrosive electrolyte and the LDX 2101 surface, implying lower corrosion tendencies.

4. Conclusions

The EGF coating was successfully prepared using a spin coater. The SEM confirms the flaky morphology, the XRD confirms the crystalline and graphitic nature and the FTIR confirms the graphitic functional group. The SEM and WCA confirm the EGF coating is rough and more water-repellent in nature. The corrosion study revealed that EGF composite has excellent corrosion protective ability compared to bare and epoxy-coated steel.

References

[1] J. Chavhan, R. Rathod, J. Malav, S. Umare, Surf. Topogr. Metrol. Prop. 8, (2020), 045029.
[2] T. Dandekar, R. Koya K S, J. Chavhan, R. Shah, R. Khatirkar, Materialia, 30, (2023), 101814
[3] O. Fayomi, I. Akande, S. Odigie J. Phys. Conf. Ser. 1378 (2019), 022037.
[4] Xiaoxu Chen, Yang Zhao, Engineering, 09 (05), (2017), 504-509
[5] Veleva L, Chin J, del Amo B, Prog. Org. Coat. 36, (1999) 211–216.
[6] N. Ismail, R. Shakoor, R. Kahraman, Prog. Org. Coat., 183, (2023), 107716.
[7] F. Jin, X. Li, S. Park, J. Ind. Eng. Chem., 29, (2015), 1-11
[8] S. Song, X. Fan, H. Yan, M. Cai, Y. Huang, C. He, M. Zhu, Composites Communications, 37, (2023), 101437.
[9] H. Lipson, A. Stokes, The structure of graphite, Proc R Soc Lond A, 181 (984), (1942), 101-105.
[10] A. Jara, J. Kim, Materials Today Communications, 25, (2020), 101437.
[11] M. Cui, S. Ren, J. Pu, Y. Wang, H. Zhao, L. Wang, Corrosion Science, 159, (2019), 108131.
[12] K. Reddy, D. Vardhan, Y. Reddy, G. Raghavendra, R. Rudrapati, Adv. Mater. Sci. Eng., 7 (2021), 3739573.
[13] Liu X, Shao Y, Zhang Y, Meng G, Zhang T, Wang F, Corrosion Science, 90, (2015) 451–462.
[14] Balaskas AC, Kartsonakis IA, Tziveleka LA, Kordas GC, Prog. Org. Coat., 74, (2012) 418–426.
[15] A. Ramya, B. Manoj, A. Mohan, Asian J. Chem.; 28 (5), (2016), 1031-1034.
[16] J. Chavhan, R. Rathod, V. Tandon, S. Gupta, J. Malav, Surf. Coat. Tech., 448, (2022) 128846.

Condition	R_s ($\Omega.cm^2$)	CPE_c ($\Omega/cm^2 S^n$)	n	R_c ($\Omega. cm^2$)	CPE_{ct} ($\Omega/cm^2 S^n$)	n	R_{ct} ($\Omega.cm^2$)

Bare	29.45	--	--	---	68.74	0.81	22672
EP	584.2	0.2843	0.98	16130	15.64	0.81	35167
EGF	2195	0.237	0.98	20265	4.472	0.74	58157

Table 1: (a) EEC Parameter obtained for bare SS, EP and EGF coated sample

Condition	E_{corr} (mV)	I_{corr} (μA)
Bare	-285.592 (±0.035)	2.689 (±0.005)
EP	-198.408 (±0.041)	0.265 (±0.004)
EGF	-117.574 (±0.026)	0.482 (±0.003)

Table 1: (b) Parameter obtained for bare SS, EP and EGF coated sample from Tafel plot

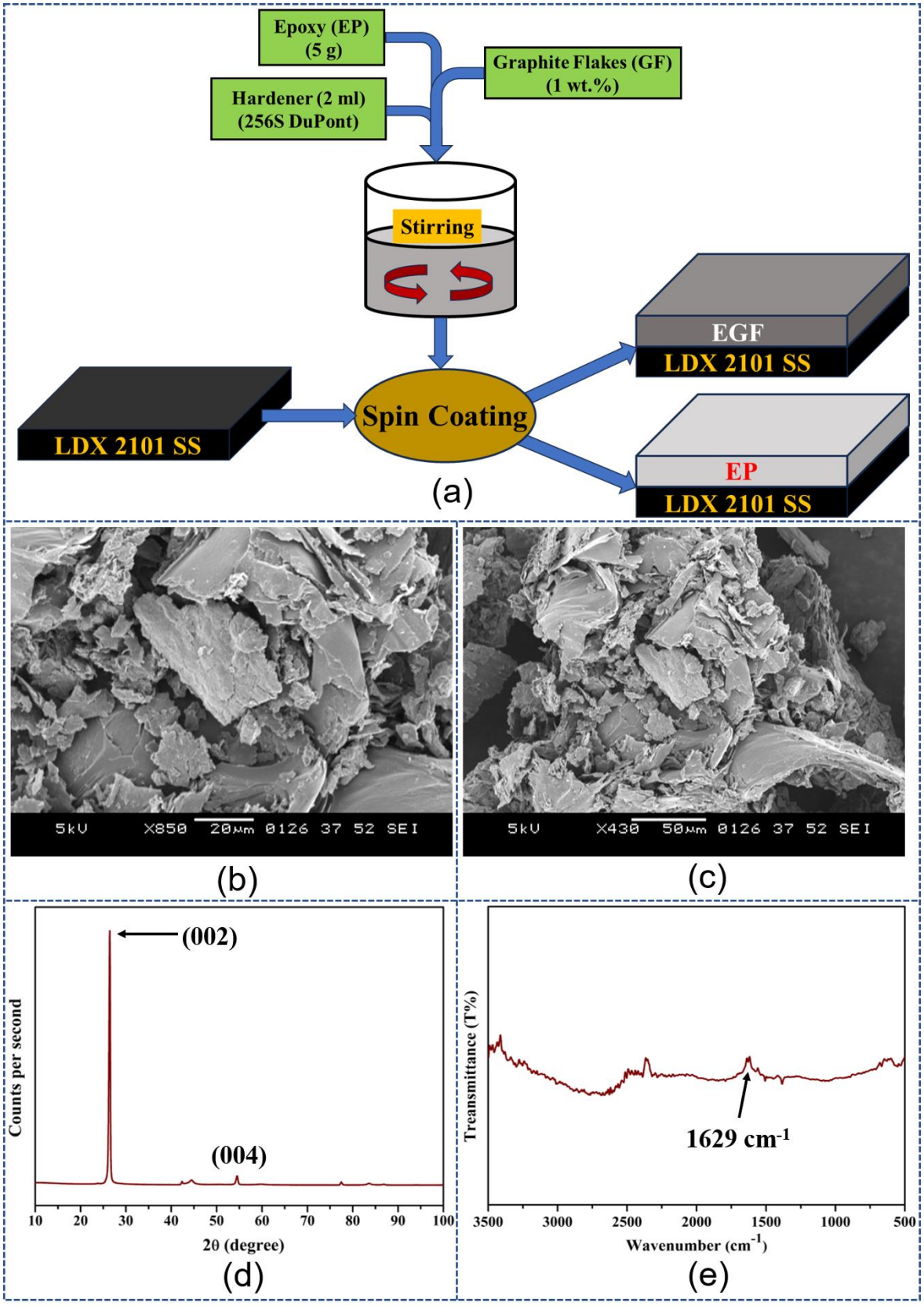

Fig. 1 (a) Schematic of fabrication of Epoxy/Graphite flakes (EGF) coating (b, c) SEM images, (d) XRD pattern and (e) FTIR spectra of graphite flakes (GF)

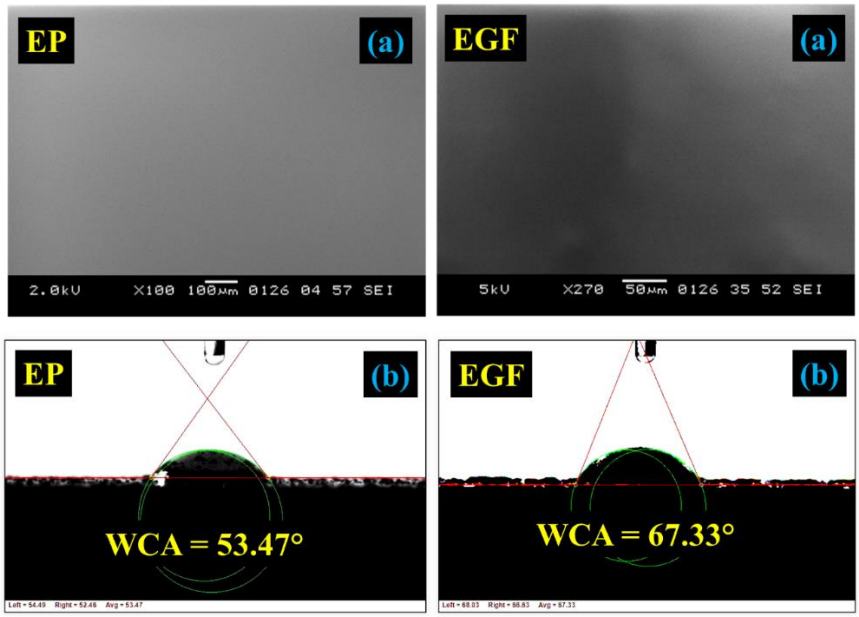

Fig. 2 (a) SEM images and (b) WCA of EP and EGF coating

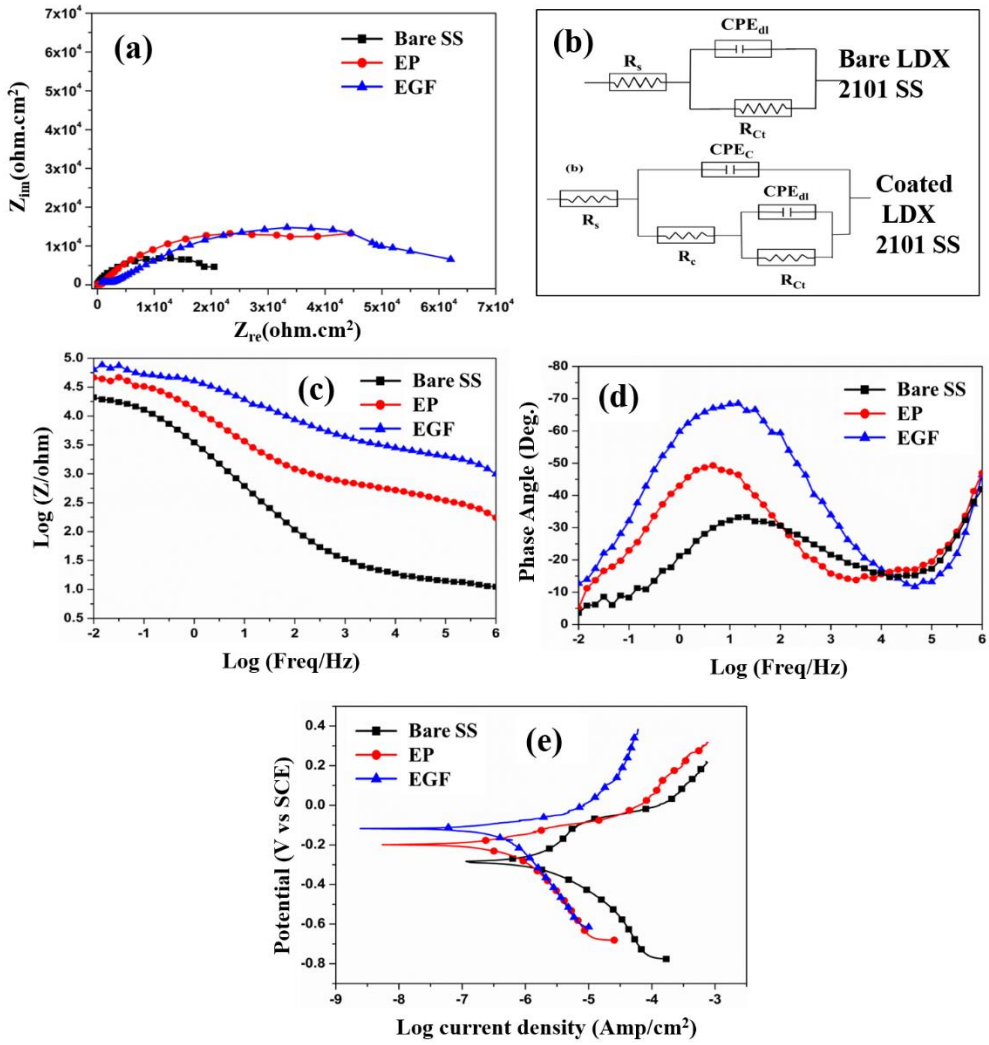

Fig. 3 (a) Nyquist plot, (b) EEC model, (c) Bode plot, (d) Phase angle plots and (e) Tafel plot of bare LDX 2101 SS, EP, EGF coated sample immersed in 3.5 % NaCl solution.